TE and TM Green's Function for Coherent and Incoherent Propagation over a Finitely Conducting Rough Surface

Akira Ishimaru, John D. Rockway, Yasuo Kuga, and Seung-Woo Lee

Department of Electrical Engineering, University of Washington, Seattle, Washington

Abstract. This paper presents wave propagation over a finitely conducting half-space whose surface is bounded by a rough surface of small rms height. An electric or magnetic current source is used to excite the rough surface and the Green's function for TE and TM wave propagation is obtained. The appearance of roughness at the boundary produces both a coherent (mean) and incoherent (fluctuating) field distribution, which is obtained from Dyson's equation and Bethe-Salpeter's equation, respectively. The coherent Green's function for vertical polarization exhibits similar characteristics to the Sommerfeld dipole problem where the Zenneck wave pole is modified by roughness. The incoherent field generated by rough surfaces is obtained for both vertical and horizontal polarization, and the conventional cross-section per unit length of the rough surface is modified to include the effects of surface roughness. For angles near grazing, a low grazing angle cross-section is obtained by evaluating the Bethe-Salpeter's equation with the Sommerfeld solution. Finally, the coherent and incoherent intensity for the TE rough surface Green's function is obtained and compared to Monte-Carlo simulations.

1. Introduction

Wave propagation over a flat conducting surface excited by a dipole is a classic electromagnetic problem and has been studied by Wait and many others [*Wait*, 1998, 1962]. In this paper, we extend the problem to include a finitely conducting medium bounded by a rough surface of small rms height ($k\sigma < 1.0$). Over the years, many investigators have considered this specific problem. Radio wave propagation over a rough surface was first studied by Feinberg [*Feinberg*, 1944] who obtained an effective impedance at the interface. Barrick conducted extensive studies on HF/VHF propagation over rough seas [*Barrick*, 1971a, b] and showed that the spherical earth residue series model should be used for MF - VHF propagation over a rough sea. This was also shown rigorously by Wait [*Wait*, 1971]. The effective impedance of a rough surface has been extensively

studied by Bass, Fuks, and others [*Bryukhovetskii et al.*, 1985; *Bass et al.*, 1979; *Bryukhovetskii et al.*, 1985] using an extension of the small perturbation theory and the diagram method [*Tatarskii*, 1967; *Rytov et al.*, 1987]. The diagram method has been applied to the rough surface scattering problem and the basic equations have been developed and solved for Dirichlet and Neumann surfaces and irregular waveguides [*Freilikher et al.*, 1970; *Bass et al.*, 1974]. Scattering by random impedance and the backscattering enhancement have been discussed using a different approach including the pole and the grazing angle considerations [*Freilikher et al.*, 1993, 1976]. Multiple scattering theories for rough surface scattering have also been proposed by Watson and Keller [*Watson et al.*, 1983, 1984], Ito [*Ito*, 1985] and Ishimaru et al.[*Ishimaru et al.*, 2000a]. Further studies have been conducted recently for LGA scattering [*Brown*, 1998; *Barrick*, 1998, 1995; *Fuks et al.*, 1999]. This paper follows and extends the multiple scattering theories developed by Bass, Fuks, Watson-Keller, Ito and Ishimaru [*Bass et al.*, 1979; *Watson et al.*, 1983, 1984; *Ito*, 1985; *Ishimaru et al.*, 2000a]. We make use of the diagram and the first order modified

perturbation method [*Tatarskii*, 1967; *Rytov et al.*, 1987; *Frisch*, 1968], to obtain an expression for the Green's function for both vertical and horizontal polarizations.

To properly consider this problem, an electric or magnetic current source excites the rough surface and can be located very near or far away from the rough surface. These two current sources will provide both vertical and horizontal polarization for wave propagation over the rough surface. When the source is located far above the surface, it is sufficient to consider a plane-wave or beam wave incident on the surface resulting in coherent (average) and incoherent (fluctuating) scattered fields radiating away from the surface.

$$G_{total}(r, r_o) = \langle G(r, r_o) \rangle + G_f(r, r_o) \qquad (1)$$

where G_{total}, $\langle G \rangle$, and G_f are the total, average, and incoherent Green's functions and r_o, r are the source and observation points. If the surface is a flat conducting surface, the incoherent field will be absent. However, for increasing roughness, the coherent field diminishes and the incoherent field will be generated and become dominant. For a source and/or observation point located near the surface, it can no longer be assumed that a real, propagating field is incident upon the surface. Instead, complex wave propagation involving both coherent and incoherent fields will excite the surface. The resulting scattered field not only includes coherent and incoherent radiation but also possibilities of complex wave propagation along the surface. To properly consider the Green's function near the surface, we allow the source and observation point to be near the surface, and consider the wave propagation along the surface in a similar manner as the Sommerfeld-Zenneck wave solution [*Ishimaru*, 1991].

The coherent field $\langle G \rangle$ for both vertical and horizontal polarization is obtained from Dyson's equations. The expression for the coherent Green's function is obtained in the spatial Fourier representation similar to the Zenneck-Sommerfeld solution. For TM propagation, the modified reflection coefficient produces a Sommerfeld pole whose location is perturbed by the roughness. The Zenneck wave pole, effective surface impedance, and attenuation function for a rough conducting surface are also obtained. The effective surface impedance is consistent with those obtained

by Feinberg [*Feinberg*, 1944], Bass and Fuks [*Bass et al.*, 1979], and Barrick [*Barrick*, 1971a, b] in appropriate limits.

To obtain the fluctuating Green's function we must consider the second moment of the field called the mutual coherence function.

$$\Gamma(r, r'; r_o, r_o') = \langle G(r, r_o) G^*(r', r_o') \rangle \qquad (2)$$

Noting (1), the mutual coherence function is given by

$$\Gamma = \Gamma_o + \Gamma_f \qquad (3)$$

where the coherent mutual coherence function is given by

$$\Gamma_o = \langle G(r, r_o) \rangle \langle G^*(r', r_o') \rangle \qquad (4)$$

which is determined from the coherent Green's function. The fluctuating or incoherent Green's function is given by

$$\Gamma_f = \langle G_f(r, r_o) G_f^*(r', r_o') \rangle \qquad (5)$$

To obtain an expression for the second moment Γ, we solve the first order Bethe-Salpeter equation under the smoothing approximation [*Wait*, 1971]. The incoherent Green's function is excited by the propagating coherent field and accumulates fluctuations from all scattering points over the surface. If we evaluate the incoherent field in the far-field, the scattering cross sections are shown to be similar to Watson-Keller [*Watson et al.*, 1983, 1984] and consistent with Fuks et al.[*Fuks et al.*, 1999] in the Neumann surface limit. Numerical Monte-Carlo simulations were conducted to compare with the bistatic cross-section for both vertical and horizontal polarizations. For source and/or field points near the surface, the complex wave propagation near the surface cannot be ignored. To compensate for the field near the surface, the Bethe-Salpeter's equation is evaluated along the surface similar to the Sommerfeld solution. A corresponding cross section near the surface is obtained and includes the Sommerfeld attenuation function and is shown to be dependent on the source location and incident grazing angle. The paper is divided as follows. In section 2, we consider the coherent Green's function and obtain expressions for both vertical and horizontal polarizations. The coherent Sommerfeld-Zenneck propagation along the surface is described for vertical polarization. In section 3, the incoherent Green's function is described. First, the far-field cross-sections are obtained from Bethe-

Salpeter's equation. Secondly, incoherent propagation along the surface is identified and a corrected cross-section near the surface is obtained. Finally in section 4, numerical Monte-Carlo simulations are conducted and compared to the total intensity of the field.

2. Coherent Green's Function

In the sections 2.1 and 2.2, we develop the formulation for TE and TM wave propagation over finitely conducting rough surfaces. At the surface, the field satisfies the impedance boundary condition where the ratio of the tangential magnetic field to the tangential electric field is the surface impedance. This effectively reduces the two-medium problem to a one-medium problem with the impedance boundary condition. Next, an equivalent boundary condition at $z = 0$ is constructed by perturbing the Green's function about the rough surface height $z = h(x)$. For both TE and TM, the random height contribution to the boundary condition, which is called the random surface potential V, is obtained. Next, by making use of Green's theorem, a random surface integral equation is formulated for the rough surface Green's function. Finally, the coherent field is obtained from Dyson's equation by averaging the random surface integral equation.

2.1. Equivalent Boundary Condition for TE and TM

Let us consider a line source located at x_o, z_o in free space above a finite conducting half-space with permitivity ϵ and conductivity σ. This half-space is bounded by a rough surface at $z = h(x)$ where $h(x)$ is a random function of the surface height, (Figure 1). The Green's function satisfies
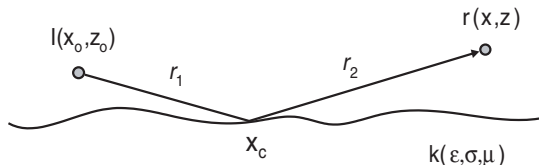
Figure 1. Magnetic or Electric line current source I is located at (x_o, z_o). Conducting medium with wave number κ, dielectric constant ϵ, conductivity σ, and permeability μ is bounded by rough surface given by the height $h = h(x)$.

$$(\frac{\partial^2}{\partial x^2} + \frac{\partial^2}{\partial z^2} + k_o^2)G(x, z) = -\delta(x - x_o)\delta(z - z_o)$$
(6)

at $z = h(x)$ where k_o is the free space wave number and satisfies the impedance boundary condition

$$G + \beta_o \frac{\partial}{\partial n}G = 0$$
(7)

where $\beta_o = -i\frac{Z_s}{k_o Z_o}$ for TE and

$$\frac{\partial}{\partial n}G + \alpha_o G = 0$$
(8)

where $\alpha_o = ik_o\frac{Z_s}{Z_o}$ for TM.

The constants $Z_o = \sqrt{\frac{\mu}{\epsilon_o}}$ are the free space characteristic impedance, $\frac{\partial}{\partial n}$ is the normal derivative, and the surface impedance Z_s is approximated by that of the flat conducting surface [*Wait*, 1998; *Bass et al.*, 1979] given by

$$Z_s = \frac{Z_o}{n}\sqrt{1 - \frac{k_x^2}{(k_o n)^2}} = Z_o\Delta$$
(9)

where $n^2 = \epsilon + i\frac{\sigma}{w\epsilon_o}$ is the refractive index of the conducting medium. Notice, if near low grazing angle $k_x \rightarrow k_o$, we can then approximate the surface impedance as $Z_s \approx \frac{Z_o}{n}\sqrt{1 - \frac{1}{n^2}}$ which for large $|n| >> 1$ reduces to $Z_s \approx \frac{Z_o}{n}$. These expressions describe the total radiation field for a line source in the presence of a half-space rough surface. If the line source is an electric current I_e, then the y-component of the electric field (TE) is given by

$$E_y(x, z) = iw\mu_o I_e G(x, z)$$
(10)

and the impedance boundary condition (7) holds. However, if the line source is a magnetic current I_m, the y-component of the magnetic field is

$$H_y(x, z) = iw\epsilon_o I_m G(x, z)$$
(11)

then the impedance boundary condition (8) holds. The fields must satisfy the boundary conditions (7),(8) at the rough surface $z = h(x)$. However, we can write an equivalent expression for the boundary condition at $z = 0$ by writing the Green's function as a perturbation expansion about $z = 0$ and including only the first-order powers of $h(x)$. We note that,

$$\frac{\partial}{\partial n} \approx -\frac{\partial h}{\partial x}\frac{\partial}{\partial x} + \frac{\partial}{\partial z} + ...$$

and

$$G(x,z) = G(x,o) + h(x)\frac{\partial}{\partial z}G + ...$$

Therefore, the equivalent surface impedance boundary condition at $z = 0$ for the Green's function is now

$$G + \beta_o\frac{\partial}{\partial z}G + V_{TE}G = 0 \qquad (12)$$

for TE and

$$\frac{\partial}{\partial z}G + \alpha_o G + V_{TM}G = 0 \qquad (13)$$

for TM. Note, the surface potential $V(x)$ is a random function of the surface height and for TE and TM is given by

$$V_{TE} = \beta_o(h\frac{\partial^2}{\partial z^2} - \frac{\partial h}{\partial x}\frac{\partial}{\partial x}) + h\frac{\partial}{\partial z} \qquad (14)$$

$$V_{TM} = h\frac{\partial^2}{\partial z^2} - \frac{\partial h}{\partial x}\frac{\partial}{\partial x} + \alpha_o h\frac{\partial}{\partial z} \qquad (15)$$

From Green's theorem we can now derive the random integral equation for the rough surface Green's function.

By making use of the surface potentials (Eq. 14 or 15), and the flat, half-space Green's function given in spectral domain as

$$G_o(r,r_o) = \frac{1}{2\pi}\int\frac{i}{2k_z}\left(e^{ik_z|z-z_o|} + R_o e^{ik_z(z+z_o)}\right)e^{i\kappa(x-x_o)}d\kappa \quad (16)$$

where the reflection coefficient for TE and TM are given by

$$R_o^{TE}(\kappa) = \frac{Q_o(\kappa) - 1}{Q_o(\kappa) + 1} \quad \text{where} \quad Q_o = i\beta_o k_z \quad (17)$$

$$R_o^{TM}(\kappa) = \frac{1 - Q_o(\kappa)}{1 + Q_o(\kappa)} \quad \text{where} \quad Q_o = \frac{\alpha_0}{ik_z} \quad (18)$$

and satisfying the impedance boundary condition

$$G_o + \beta_o\frac{\partial}{\partial z}G_o = 0 \qquad (TE) \qquad (19)$$

$$\frac{\partial}{\partial z}G_o + \alpha_o G_o = 0 \qquad (TM) \qquad (20)$$

we can obtain the random surface integral equation [Bass et al., 1979; Ishimaru et al., 2000a, b]

$$G(r,r_o) = G_o(r,r_o) + \int G_o(r,r_1)V(r_1)G(r_1,r_o)dx_1 \qquad (21)$$

where $r = r(x,z), r_o = r_o(x_o,z_o)$, and $r_1 = r_1(x_1, z_1 = 0)$. G_o is the flat, half-space Green's func-

tion and is a deterministic function, while the surface potential $V(r_1)$ and the rough surface Green's function $G(r,r_o)$ are random functions. From (21), we can generate the higher order moments describing the propagation such as the coherent field and incoherent intensity. By using the diagram method, we can obtain Dyson's equation for the coherent Green's function [Bass et al., 1979]

$$\langle G(r,r_o)\rangle = G_o(r,r_o) + \int G_o(r,r_1)\mathcal{M}(r_1,r_2)$$
$$\langle G(r_2,r_o)\rangle dx_1 dx_2 \quad (22)$$

where the Mass operator under the first-order smoothing approximation [Frisch, 1968] is given by $\mathcal{M}(r_1,r_2) = \langle V(r_1)G_o(r_1,r_2)V(r_2)\rangle = \mathcal{M}(r_1 - r_2)$. We note that the correlation function of the random surface potential $V(x)$ is related to the correlation function of the rough surface height $h(x)$. We can express the height correlation as

$$\langle h(x_1)h(x_2)\rangle = \int W(\kappa)e^{i\kappa(x_1-x_2)}d\kappa \qquad (23)$$

where we assumed $h(x)$ is a homogeneous random function and $W(\kappa)$ is the power spectral density function. In this paper, we use the Gaussian correlation function for $h(x)$ with rms height h_o and correlation distance l.

$$\langle h(x_1)h(x_2)\rangle = h_o^2 e^{-\frac{(x_1-x_2)^2}{l^2}} \qquad (24)$$
$$W(\kappa) = \frac{h_o^2 l}{2\sqrt{\pi}}e^{-\frac{\kappa^2 l^2}{4}}$$

The Gaussian spectrum is used to verify our analytical results by comparing with numerical Monte-Carlo simulations based on the Gaussian spectrum. It should be noted, however, that our results can be used for any spectrum which would be used to represent an actual problem.

2.2. Coherent Field, Sommerfeld Pole and Zenneck Wave for Conducting Rough Surfaces

In this section, we solve Dyson's equation [Ishimaru et al., 2000b] to obtain the coherent Green's function $\langle G\rangle$. For TM propagation there exists a pole contribution which is used to calculate the Zenneck wave. However, for TE there is no pole. To solve Dyson's equation, we write the coherent Green's function in the spectral domain as

$$\langle G(r,r_o)\rangle = \frac{1}{2\pi}\int\frac{i}{2k_z}\left(e^{ik_z|z-z_o|} + R(\kappa)e^{ik_z(z+z_o)}\right)e^{i\kappa(x-x_o)}d\kappa \quad (25)$$

By making use of the flat surface Green's function (16), the coherent Green's function (25), and the height correlation (23), we can obtain from Dyson's Eq. (22) the TE reflection coefficient

$$R^{TE}(\kappa) = \frac{Q(\kappa) - 1}{Q(\kappa) + 1} \qquad (TE) \qquad (26)$$

where

$$Q(\kappa) = \frac{Q_o(\kappa) + ik_z \int L(\kappa', \kappa)W(\kappa - \kappa')d\kappa'}{1 - ik_z \int L(\kappa', \kappa)W(\kappa - \kappa')\beta_o M(\kappa, \kappa')d\kappa'} \qquad (27)$$

$$L(\kappa, \kappa') = \frac{[\beta o(\kappa\kappa' - k^2)Q_o(\kappa') - ik_z']}{1 + Q_o(\kappa')}$$

$$M(\kappa, \kappa') = \frac{i}{k_z}(\kappa\kappa' - k^2)$$

and the TM reflection coefficient,

$$R^{TM}(\kappa) = \frac{1 - Q(\kappa)}{1 + Q(\kappa)} \qquad (TM) \qquad (28)$$

where

$$Q(\kappa) = \frac{Q_o(\kappa) - \int L_1(\kappa', \kappa)W(\kappa - \kappa')M_2(\kappa, \kappa')d\kappa'}{1 + \int L_1(\kappa', \kappa)W(\kappa - \kappa')\alpha_o d\kappa'} \qquad (29)$$

$$L_1(\kappa', \kappa) = \frac{M_1(\kappa', \kappa) + \alpha_o Q_o(\kappa')}{1 + Q_o(\kappa')}$$

$$M_1(\kappa', \kappa) = \frac{i}{k_z'}[\kappa\kappa' - k_o^2]$$

$$M_2(\kappa, \kappa') = \frac{i}{k_z}[\kappa\kappa' - k_o^2]$$

The effective surface impedance obtained from Q in (26)-(29) are special cases of the more general cases discussed in [*Bass et al.*, 1979]. The first thing to note, is that the coherent field $\langle G \rangle$ behaves in exactly the same manner as the deterministic flat surface Green's function G_o. The difference lies in the description of the reflection coefficient. In fact, the coherent Green's function can reduce to the flat surface Green's function by allowing the surface height to go to zero $z \to 0$ causing $Q(\kappa) \to Q_o$ which reduces to the flat surface. Secondly, the impedance boundary condition reduces to Dirichlet's condition by allowing $\beta_o \to 0$, $Q_o = 0$ and $R_o^{TE} = -1$

$$R_{Dir}(\kappa) = \frac{Q(\kappa) - 1}{Q(\kappa) + 1},$$

$$Q(\kappa) = k_z \int k_z' W(\kappa - \kappa')d\kappa' \qquad (30)$$

and Neumanns condition by allowing $\alpha_o \to 0$, $Q_o = 0$ and $R_o^{TM} = 1$.

$$R_{Neu}(\kappa) = \frac{1 - Q(\kappa)}{1 + Q(\kappa)},$$

$$Q(\kappa) = \int M_1(\kappa', \kappa)M_2(\kappa, \kappa')W(\kappa - \kappa')d\kappa' \qquad (31)$$

These two cases have also been obtained by Watson and Keller [*Watson et al.*, 1983, 1984]. For the TM case, we can calculate the effective surface impedance for the coherent field

$$\overline{\Delta(\kappa)} = \frac{k_z}{k_o}Q(\kappa) \qquad (32)$$

Noting that $\Delta = \frac{k_z}{k_o}Q_o(\kappa)$, and in the limit as $\alpha_o \to 0$,

$$\overline{\Delta(\kappa)} = \Delta - \frac{k_z}{k_o} \int M(\kappa', \kappa)W(\kappa - \kappa')M(\kappa, \kappa')d\kappa'$$

which agrees with Barrick [*Barrick*, 1971a, Eq. (24)] when converted to the one-dimensional surface and evaluated at $\kappa = k_o$.

The coherent Green's function for vertical polarization in the far-field maybe evaluated using the saddle-point asymptotic technique and is given by

$$\langle G(r, r_o) \rangle \overset{kR \to \infty}{=\!=\!=} G_p(R_1) + R^{TM}(\theta^s, \theta^i)G_p(R_2),$$

$$\theta^s = \theta^i, \quad R_2 = r_1 + r_2$$

However, of interest is when the source and observation points near the surface for vertical polarization. If we consider complex propagation along the surface, and evaluate the coherent Green's function using the modified saddle-point technique which takes into account the Zenneck pole, we arrive at

$$\langle G(r, r_o) \rangle = G_p(R_1) + G_p(R_2) - 2\langle P \rangle \qquad (33)$$

where

$$G_p(R) = \frac{i}{4}H_o^{(1)}(k_o R) \approx \frac{1}{4}\left(\frac{2}{\pi k_o R}\right)^{1/2}e^{ikR + i\pi 4} \qquad (34)$$
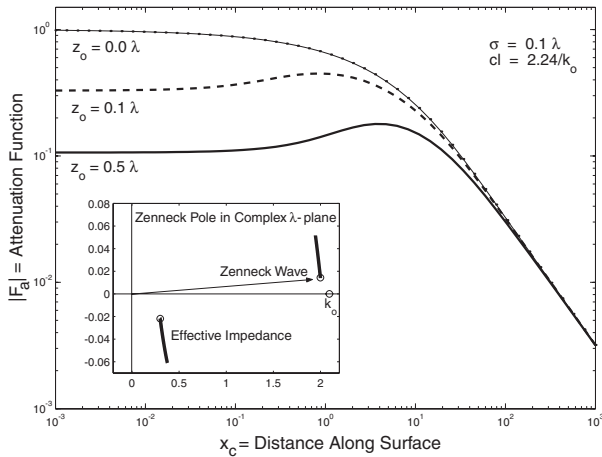
represents the direct and image source and

$$\langle P \rangle = G_p(R_2)[-i\sqrt{\pi p}\ e^{-p}erfc(-i\sqrt{p}\ )] \qquad (35)$$

represents scattering from along the surface. Now the numerical distance p is the difference between the total phase for the Zenneck wave and free space

$$p = ikR_2 - i[\kappa(x - x_o) + k_z(z + z_o)] \qquad (36)$$

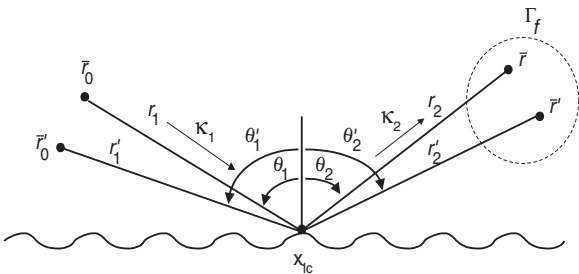where the propagation constant for the Zenneck wave must be determined from the pole.

$$1 + Q(\kappa) = 0 \qquad (37)$$

Figure 2. Attenuation function F_a as a function of distance x_c along the surface for given heights z_o of source above the surface. Also included within the insert is the complex λ- plane showing the trend of the Zenneck pole and surface impedance for increasing rms heights. Distances are in unit of wavelength, and the ground dielectric constant is $10 + 5i$.

By solving Dyson's equation for the rough surface field, we achieve a new reflection coefficient, a new Sommerfeld pole and finally the new Zenneck wave different from the flat surface. The final form of the solution is identical to that for the deterministic case, but the Sommerfeld pole has been re-positioned due to roughness. In order to calculate the propagation constant for the Zenneck wave, we first calculate k_z from (29) and (37), which we can express as the following

$$k_z = \frac{-k_o\Delta}{1 - \int L_1(\kappa', \kappa)W(\kappa - \kappa')[M_2(\kappa, \kappa') - \alpha_o]d\kappa'} \quad (38)$$

Figure 3. Incoherent intensity and scattering cross section.

Notice, for the flat surface case, $k_z = -k_o\Delta$. Therefore, the integral in (38) represents the rough surface effects. The propagation constant for the Zenneck wave is then obtained by

$$\kappa = \sqrt{k_o^2 - k_z^2} \quad (39)$$

For source and field points located near the surface $zo \approx z \approx 0.0$, the rough surface Green's function reduces to

$$\langle G(r, r_o)\rangle = 2G_p(R)F(p) \quad (40)$$

where $F(p)$ is the attenuation function of the field along the surface and is given by

$$F(p) = 1 + i\sqrt{\pi p}\, e^{-p} erfc(-i\sqrt{p}\,) \quad (41)$$

In Figure 2, we plot the attenuation function for varying heights of the source above the rough surface with rms height ($\sigma = .1\lambda$). The insert in the figure shows the behavior of the pole, and the effective impedance in the complex λ-plane as the rms height increases. In general, the behavior of the pole is to became more attenuative.

3. Incoherent Intensity

Let us now consider the second moment of the field or the incoherent intensity. For small surface roughness, the coherent field will dominate. However, as the roughness increases, or at larger distances from the surface, the coherent field diminishes and the incoherent intensity becomes dominant. The incoherent intensity is obtained from the first-order Bethe-Salpeter equation which describes the Mutual Coherence function or the correlation of fields at r and r' due to the sources located at r_o and r'_o (Figure 3). The MCF may be written as the sum of coherent and incoherent intensity

$$\Gamma(r, r'; r_o, r'_o) = \langle G(r, r_o)G^*(r', r'_o)\rangle = \Gamma_o + \Gamma_f \quad (42)$$

where the coherent intensity was determined from section 2.2

$$\Gamma_o = \langle G(r, r_o)\rangle\langle G^*(r', r'_o)\rangle \quad (43)$$

and the fluctuating intensity is given by the first iteration of the Bethe-Salpeter's equation.

$$\Gamma_f = \int \langle G(r, r_1)\rangle\langle G^*(r', r'_1)\rangle\langle V(r_1)V(r'_1)\rangle$$
$$\langle G(r_1, r_o)\rangle\langle G^*(r'_1, r'_o)\rangle dr_1 dr'_1 \quad (44)$$

Since the coherent Green's function $\langle G\rangle$ has been determined (25), we can then evaluate the Bethe-

Salpeter equation in the far field [*Ishimaru et al.*, 2000a] to determine the incoherent intensity.

$$I_f = 4k_o \int dx_c |G_o(r, r_1)|^2 |G_o(r_1, r_o)|^2 \sigma^o(\kappa, \kappa_1) \tag{45}$$

where σ^o is the scattering cross-section per unit length of the finitely conducting rough surface. κ and κ_1 are the wave numbers corresponding to the vectors $r - r_1$ and $r_1 - r_o$ respectively. The cross section for the TM case is given by

$$\sigma^o = \frac{2\pi}{k_o} \frac{4 |\kappa_s \kappa_1 - \kappa_{1z}^2 - i\kappa_{1z}\alpha_o Q(\kappa_1)|^2}{|1 + Q(\kappa)|^2 |1 + Q(\kappa_1)|^2} \cdot W \tag{46}$$

and for TE

$$\sigma^o = \frac{2\pi}{k_o} \frac{4 |\beta_o(-k_{z1}^2 + \kappa_s \kappa_1) Q(\kappa_1) - ik_{z1}|^2}{|1 + Q(\kappa)|^2 |1 + Q(\kappa_1)|^2} |k_z|^2 \cdot W \tag{47}$$

where $W = W(\kappa - \kappa_1)$ is the power spectral density function and $\kappa_s = \kappa - \kappa_1$. For the Neumann surface, $\alpha_o = 0$ the cross-section reduces to a similar expression of Fuks et al. [*Fuks et al.*, 1999].

Of particular interest is the ratio of crosssections HH/VV in the back-direction, as the angle of incidence approaches grazing angle. We first consider the perfecly conducting rough surface and Dirchlet's (HH) and Neumann's (VV) boundary condition. It should be noted that for the first order small perturbative method (SPM), the ratio of HH/VV predicts very little backscattering.

$$SPM \sim HH/VV = \frac{|k_{zi}|^4}{|\kappa_i^2 + k_o^2|^2}$$

which as the grazing angle approaches zero $\theta_g \to 0$, $k_z \to 0$ and therefore

$$SPM \sim HH/VV \approx \emptyset$$

Also, of note, the ratio HH/VV for SPM is independent of any rough surface parameters (i.e. rms height σ and correlation length cl) and is only dependent on the incident angle. If we now consider the ratio of HH/VV given in Eq. 46 and 47, for Dirchlet's and Neumann's condition ($\beta_o = 0, \alpha_o = 0$), the corresponding ratio becomes

$$Ishimaru's \sim HH/VV =$$
$$\frac{|k_{zi}|^4}{|\kappa_i^2 + k_o^2|^2} \cdot \frac{|1 + Q^V(\kappa_i)|^2}{|1 + Q^H(\kappa_i)|^2} \frac{|1 + Q^V(-\kappa_i)|^2}{|1 + Q^H(-\kappa_i)|^2} \tag{48}$$
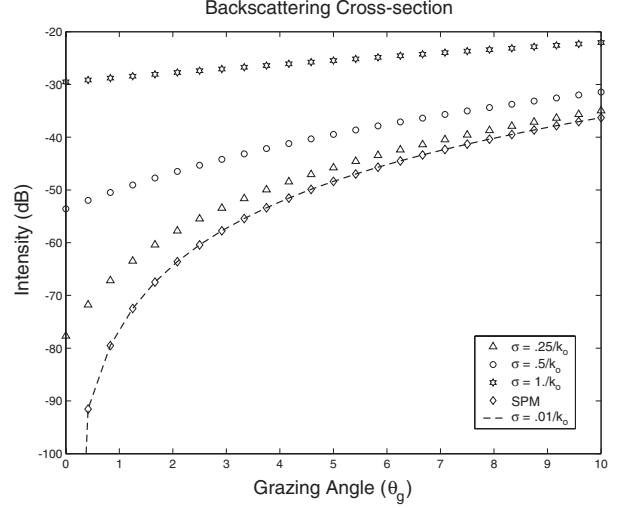
Figure 4. Ratio of HH/VV for Backscattering Cross-section σ^{HH}/σ^{vv} as a function of grazing angle from $0.5^o \sim 10^o$ for a perfectly conducting rough surface. Comparison of SPM and (48) for several different rms heights and correlation length $cl = 2.24/k_o$.

where the reflection coefficients are given by (30) with

$$Q^H(\kappa) = k_z \int k_z' W(\kappa - \kappa') d\kappa'$$

and

$$Q^V(\kappa) = \frac{1}{k_z} \int \frac{(k_o^2 - \kappa\kappa')^2}{k_z'} W(\kappa - \kappa') d\kappa'$$

Due to the surface spectrum $W(\kappa - \kappa')$, the ratio of HH/VV will have some rough surface dependence. In Figure 4, we plot the ratio of HH/VV in the back-direction for a perfectly conducting surface and compare SPM to Eq. 48, for grazing angles ranging from $.001^o \sim 10^o$. Shown in the figure, the SPM result is independent of rough surface parameters, and goes to zero as grazing angle approaches zero. However, our results predict a finite intensity that is dependent on the rms height of the rough surface. The results are all based upon the first order scattering theory.

We now consider the impedance boundary condition or finite ground. If we evaluate the ratio of HH/VV in the back-direction near grazing angles for SPM [*Ishimaru*, 1997], then SPM predicts a finite return due to the presence of the finite ground. Also, if we go ahead and calculate the ratio of HH/VV given by Eq. 46 and 47, near grazing angle, in a straightfor-

ward manner we get

$$HH/VV = \frac{|\beta_o(\kappa_i^2 + k_o^2)Q(\kappa_i) + ik_{zi}|^2 k_{zi}^2}{|\kappa_i^2 + k_o^2 + i\kappa_{iz}\alpha_o Q(\kappa_i)|^2}$$
$$\cdot \frac{|1 + Q^V(\kappa_i)|^2}{|1 + Q^H(\kappa_i)|^2} \frac{|1 + Q^V(-\kappa_i)|^2}{|1 + Q^H(-\kappa_i)|^2} \quad (49)$$

However, let us re-consider the evaluation of the vertical cross-section (46), as the angle of incidence approaches grazing angle and the source and observation points near the surface. Normally, we would try to evaluate the vertical cross section for grazing angles, by restricting $k_x \to k_o$ as $\theta^i \to \pi/2$. However, after careful analysis of (46) and the generating incoherent MCF (44), two noticeable conflicts can be seen as we approach field points near the surface. First, the evaluation of the cross section from (44) was conducted through a far-field approximation. This approximation can only be valid for moderate angles of incidence and becomes inappropriate as $\theta \to \pi/2$. Secondly, in the evaluation of the coherent Green's function, we restricted the scattering to real propagating modes. However, from the analysis of the coherent Green's function in section 2.2, we see that complex wave propagation becomes unavoidable as we near the surface. Thus to overcome these obstacles, we evaluate the coherent Green's function for vertical polarization in (44), in a similar manner to the surface wave propagation where $\langle G \rangle = G_p(R_1) + G_p(R_2) - 2\langle P \rangle$. In doing so, we restrict our source and receiver to being near the surface (Figure 1) and thus the modified incoherent Green's function for low grazing angle becomes

$$I_f = 4k_o \int dx_c |G_o(r, r_o)|^2 \sigma_{LGA}^o(\kappa, \kappa_1) |G_o(r_1, r_o)|^2 \quad (50)$$

where

$$\sigma_{LGA}^o = \frac{2\pi}{k_o} 4 |\kappa_s \kappa_1 - \kappa_{1z}^2 - i\kappa_{1z}\alpha_o Q(\kappa_1)|^2$$
$$|F_a(R_1)F_a(R_2)|^2 W(\kappa - \kappa_1) \quad (51)$$

and F_a is the attenuation function for the TM case (41). Noticeably, the only difference in the cross-section expressions lies in the difference between $1 + Q(\kappa)$ in the far field and $F(R)$ near the surface. However, closer examination of (51) reveals the position dependence of the source and scattering center x_c of the rough surface. The scattering center is the location at which the incoherent scattering is localized. By varying it, we can vary the amount of attenuation of the field along the surface.
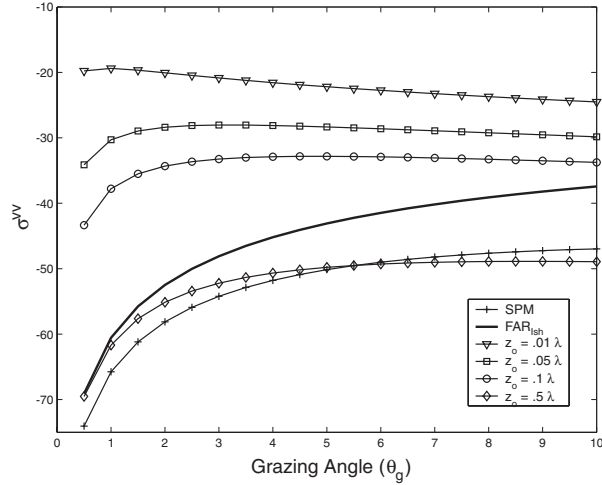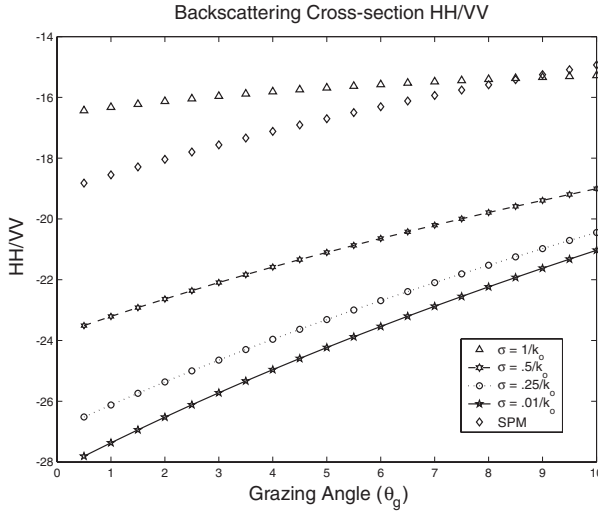

Figure 5. Cross-section σ^{vv} as a function of grazing angle from $0.5^o \sim 10^o$ for a finite conducting rough surface ($\epsilon = 10 + 5i$) with correlation length $cl = 2.24/k_o$. Compares results from SPM, Ishimaru et al.'s Far-Field cross-section (46) [*Ishimaru et al.*, 2000b] and the LGA cross-section (51). The LGA cross-section includes several different possible source heights.

Thus, the relationship between the low grazing angle $\theta_g(= \pi/2 - \theta_i)$, the source height, and the scattering center x_c is given by

$$tan(\theta_g) = \frac{z_o}{x_c}$$

In Figure 5, the low-grazing angle backscattering cross-section for vertical polarization is calculated from the attenuation function of Figure 2, for varying source heights as a function of grazing angle from $\theta_g = .5^o - 10^o$. As the source point and observation points near the surface, the grazing angle goes to zero, and the corresponding LGA cross section increases. The LGA cross-section is shown for three different source heights above the surface ($z_o = .1\lambda, .25\lambda$ and $.5\lambda$). Included within the figure, are the far-field vertical cross section (46) and the SPM cross section. Beyond a certain source height ($z_o \approx .75\lambda$), the LGA cross section is invalid, and the far-field cross-section (46) should be used instead. In Figure 6, we plot the ratio of HH/VV in the back-direction for SPM compared to our far-field cross-section approximation (49). As can be seen, the SPM produces a finite intensity and once again is independent of the rough surface parameters. Our results show much more deviation due to the rough surface height dependence. In Figure 7, we compare

Figure 6. Ratio of HH/VV for Backscattering Cross-section σ^{HH}/σ^{vv} as a function of grazing angle from $0.5^o \sim 10^o$ for the finite conducting case with correlation length $cl = 2.24/k_o$.

the SPM results to the far field cross-section (49) and the ratio of HH/VV which makes use of the vertical near field LGA cross-section (51) for two rough surface heights $\sigma = .5/k_o$ and $\sigma = 1./k_o$. The source height for the LGA cross-section are chosen to be $z_o = .1\lambda, .25\lambda$ and $.5\lambda$. The arrows point from the LGA cross-section to the far-field cross-section of similiar rough surface height cases.

4. Rough Surface Green's Function

In this section, we add together both coherent and fluctuating fields to construct a picture of the scattering process occuring when a line source excites the rough surface. The rough surface Green's function must be constructed in a second-order sense, due to the second-order nature of the incoherent Green's function. If we consider the intensity, then the rough surface Green's function is given by

$$\langle |G(r, r_o)|^2 \rangle = |\langle G(r, r_o) \rangle|^2 + \langle |G_f(r, r_o)|^2 \rangle \quad (52)$$

where the coherent Green's function intensity was given in section 2, and the fluctuating Green's function from section 3. Having noticed the complex propagation near the surface and the real propagating modes away from the surface, the Green's function must be constructed in such a manner that the
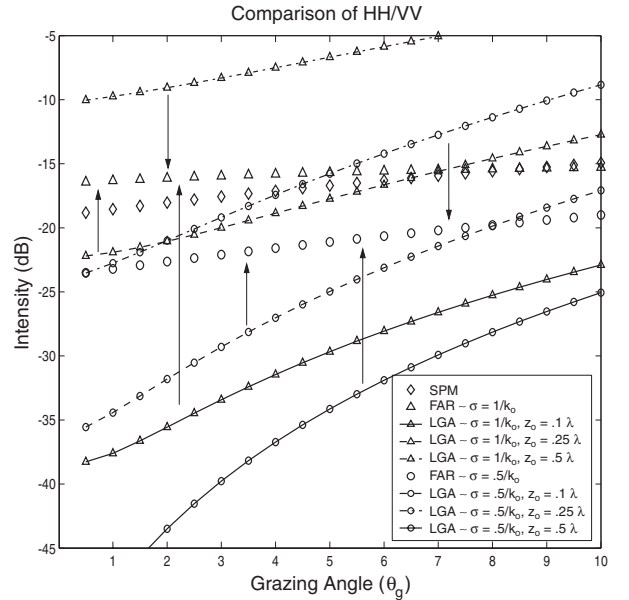
Figure 7. Ratio of HH/VV for Backscattering Cross-section σ^{HH}/σ^{vv} as a function of grazing angle from $0.5^o \sim 10^o$. Comparison of SPM, Far-Field approximation (49) and LGA cross-section (51). The arrows point from the LGA case to the Far-Field case of similiar rms height.

approximation must be determined best suited for a region of interest. For instance, if the source and observation points are near the surface, then the surface wave and LGA cross-section must be used for the coherent and incoherent fields, respectively. If the observation and field points are away from the source, then we can simply consider the far-field approximations for both coherent and incoherent fields. Finally, if the mixed propagation occurs, where the source is near and the observation point is far, what is the scattering process. Since the incident source is near the surface, the surface wave Green's function must be used to excite the surface. The corresponding cross-section, however is a mixture of complex wave and real propagation. From the earlier analysis, the cross-section was modified by the attenuation function F_a for field points near the surface, and the factor $1 + Q(\kappa)$ in the far field. Therefore, since the incident field is near the surface and the scattered field away from the surface, the corresponding cross-section makes use of a $|F_a(R_1)|$ for the incident wave and a $1 + Q(\kappa)$ for the scattered wave. Therefore,

Total Intensity → $\langle |G|^2 \rangle$

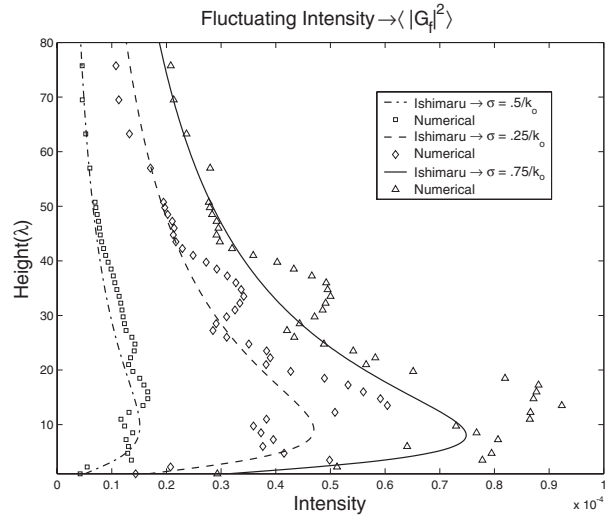Fluctuating Intensity → $\langle |G_f|^2 \rangle$
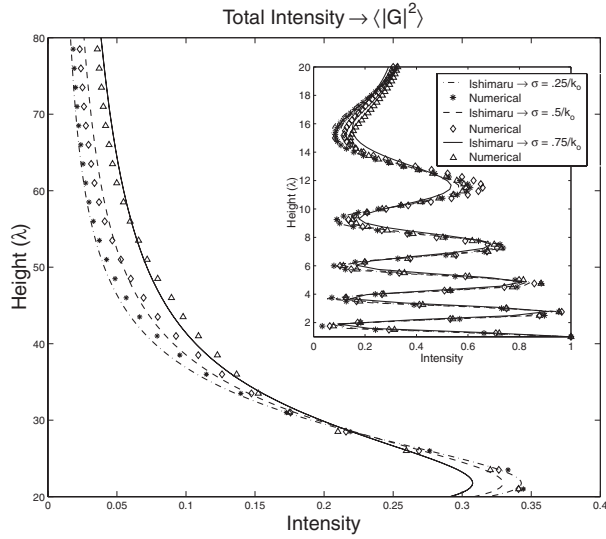
Figure 8. TE Propagation: Total rough surface Green's function intensity (Eq.52) vs. numerical simulation. The source is located at $(x_o, z_o) = (0.0\lambda, 3\lambda)$ and observation point at $x = 10\lambda$. The vertical position of the source ranges from $1 \sim 20\lambda$ above the surface (as shown in insert) and $20 - 80\lambda$ (in main plot). The correlation length is $cl = 2.24/k_o$ and three different rms heights $\sigma = .25/k_o, .5/k_o$ and $.75/k_o$ are shown.

Figure 9. TE Propagation: Incoherent Green's function intensity vs. numerical simulation for the cases shown in Fig.8.

ulations have variations, which should diminish as the number of realizations are increased.

5. Conclusions

In this paper, we discussed the effects of surface roughness on the Sommerfeld propagation problem for a conducting surface. With a rough surface, the field consists of the coherent and the incoherent field. The technique is based on the modified perturbation method and Dyson's equation. The expressions for the new Sommerfeld pole, Zenneck wave, numerical distance, and propagation factors are obtained; numerical examples are conducted; and the analytical results are compared with Monte-Carlo simulations. We then considered the incoherent mutual coherent function and gave a general expression. We also obtained the expression for the scattering cross-section per unit length of the rough conducting surface. For large grazing angles , we use the far-field cross-section (46) and (47). However, as we approach LGA, we make use of the low grazing angle cross-section (51) for vertical polarization, in which we can incorporate source position and grazing angle.

this mixed propagation crosssection can be given as

$$
\begin{aligned}
\sigma_{LGA}^o &= \frac{2\pi}{k_o} 4 \left| \kappa_s \kappa_1 - \kappa_{1z}^2 - i\kappa_{1z}\alpha_o Q(\kappa) \right|^2 \\
&\quad \frac{|F_a(R_1)|^2}{|1 + Q(\kappa_1)|^2} W(\kappa - \kappa_1)
\end{aligned}
\tag{53}
$$

. In a similar manner for the other propagation path, where the source is far from the surface, and the observation near the surface, the corresponding cross-section can be computed. In Figure 8 and Figure 9, we construct the intensity of the Green's function and compare to Monte-Carlo simulations for the TE propagation case. The source and observation points were chosen as $x_o = 0.0\lambda, z_o = 3\lambda, x = 10\lambda$, and the observation points z were allowed to vary from $0.0 - 50\lambda$. The rough surface heights chosen were for rms height $\sigma = .25/k_o, .5/k_o$, and $.75/k_o$ with correlation length $2.24/k_o$. Notice, as the rms height increases, the incoherent Green's function begins to increase. Thus for a given source and observation position, the rough surface Green's function for small rms heights maybe constructed and compares well with the Monte-Carlo simulations. Note that because of a limited number of realizations, the sim-

References

Wait, J. R., The ancient and modern history of EM ground-wave propagation, *IEEE Antennas and Propag. Mag.*, *40*(5), 7-24, October, 1998.

Wait, J. R., *Waves in Stratified Media*, Pergamon, Tarrytown, N.Y. 1962.

Feinberg, E., On the propagation of radio waves along an imperfect surface, *J. Phys. (Moscow)*, *8*, 317-330, 1944.

Barrick, D. E., Theory of HF/VHF propagation across the rough sea. Part I: The effective surface impedance for a slightly rough highly conducting surface at grazing incident, *Radio Sci.*, *6*, 517-526, 1971a.

Barrick, D. E., Theory of HF/VHF Propagation across the Rough Sea. Part II: Application to HF/VHF Propagation above the Sea, *Radio Sci*, *6*, 527-533, 1971b.

Wait, J. R., Appendix C: On the Theory of Ground Wave Propagation over a Slightly Roughened Curved Earth, in *Electromagnetic Probing in Geophysics*, Golem Press: Boulder, CO, pp. 37-381, 1971.

Bryukhovetskii, A. S., and I. M. Fuks, Effective impedance tensor of a statistically uneven impedance surface, *Radiophys. Quantum Electron., 28,* 977-983, 1985.

Bass, F. G., and I. M. Fuks, *Wave Scattering for Statistically Rough Surface*, Pergamon, New York, 1979.

Bryukhovetskii, A. S., V. M. Tigrov, and I. M. Fuks, Effective impedance tensor of statistically rough ideally conducting surface, *Radiophys. Quantum Electron., 27,* 703-708, 1984.

Tatarskii, V. I., *Wave propagation in a Turbulent Medium*, New York: Dover Publications, Inc., 1967.

Rytov, S. M., Yu. A. Kravtsov, and V. I. Tatarskii, *Principles of Statistical Radiophysics*, Berlin, New York; Shpinger-Verland, 1987.

Watson, J. G., and J. B. Keller, Refection, scattering and absorption of acoustic waves by rough surfaces, *J. Acoust, Soc. Am., 74,* 1887-1894, 1983.

Watson, J. G., and J. B. Keller, Rough surface scattering via the smoothing method, *J. Acoust. Soc. Am., 75,* 1705-1708, 1984.

Ito, S., Analysis of scalar wave scattering from slightly rough random surfaces: A multiple scattering theory, *Radio Sci., 20,* 1-12, 1985.

Ishimaru, A., J. D. Rockway, Y. Kuga, Rough surface Green's function based on the first order modified perturbation and smoothing diagram method, *Waves in Random Media, 10*(1), 17-32, 2000a.

Brown, G. S., Special issue on low-grazing-angle backscattering from rough surfaces, *IEEE Trans. Antennas Propag., 46,* 1-2, 1998.

Barrick, D. E., Grazing behavior of scatter and propagation above any rough surface, *IEEE Trans. Antennas Propag., 46,* 73-83, 1998.

Barrick, D. E., Near-grazing illumination and shadowing of rough surfaces, *Radio Sci, 30,* 563-580, 1995.

Fuks, I. M., V. I. Tatarskii, and D. E. Barrick, Behavior of scattering from a rough surface at small grazing angles, *Waves in Random Media, 9*, 295-305, 1999.

Ishimaru, A., *Wave Propagation and Scattering in Random Media*, IEEE/ OUP, N.J. 1997.

Frisch, U., Wave Propagation in Random Media in *Probabilistic Methods in Applied Mathematics*, edited by A. T. Bharucha-Reid, Academic Press, N.Y. 1968.

Ishimaru, A., *Electromagnetic Wave Propagation, Radiation and Scattering*, Prentice Hall, N.Y. 1991.

Ishimaru, A., J. D. Rockway, Y. Kuga and S.-W. Lee, Sommerfeld and Zenneck wave propagation for a finitely conducting one-dimensional rough surface, *IEEE Trans. Antennas Propag., 48*(9), 1475-1484, 2000b.

Freilikher, V. D., and I. M. Fuks, Green's-function method for the Helmholtz equation with perturbed boundary conditions, *Radiophys. Quantum Electron., 13,* 73-79, 1970.

Bass, F. G., V. D. Freilikher and I. M. Fuks, Propagation in statistically irregular waveguides, *IEEE Trans. Antennas Propag., 22*(2), 278-295, 1974.

Freilikher, V., and I. Yurkevich, Backscattering enhancement from surfaces with random impedance, *Phys. Lett. A, 183,* 247-252, 1993.

Freilikher, V. D., and I. M. Fuks, Wave reflection from a rough impedance surface, *Radiophys. Quantum Electron., 19,* 281-285, 1976.